



Permeability and elastic modulus of cement paste as a function of curing temperature

John J. Valenza II ^{*}, Jeffrey J. Thomas

Schlumberger-Doll Research, One Hampshire St., Cambridge, MA 02139, USA

ARTICLE INFO

Article history:

Received 2 August 2011

Accepted 15 November 2011

Keywords:

Permeability (C)
Mechanical Properties (C)
Curing Temperature (A)
Characterization (B)

ABSTRACT

The permeability and elastic modulus of mature cement paste cured at temperatures between 8 °C and 60 °C were measured using a previously described beam bending method. The permeability increases by two orders of magnitude over this range, with most of the increase occurring when the curing temperature increases from 40 °C to 60 °C. The elastic modulus varies much less, decreasing by about 20% as the curing temperature increases from 20 °C to 60 °C. All specimens had very low permeability, $k < 0.1 \text{ nm}^2$, despite having relatively high porosity, $\phi \sim 40\%$. Concomitant investigations of the microstructure using small angle neutron scattering and thermoporometry indicate that the porosity is characterized by nanometric pores, and that the characteristic size of pores controlling transport increases with curing temperature. The variation of the microstructure with curing temperature is attributed to changes in the pore structure of the calcium–silicate–hydrate reaction product. Both the empirical Carmen–Kozeny, and modified Carmen–Kozeny permeability models suggest that the tortuosity is very high regardless of curing temperature, $\xi \sim 1000$.

© 2011 Elsevier Ltd. All rights reserved.

1. Introduction

The hydration of portland cement results in the precipitation of product phases onto the surface of the unhydrated cement grains. These products grow into the capillary pore space, originally occupied by the mix water, decreasing the volume and connectivity of the intergranular porosity. The most important product phase for setting and hardening is the calcium silicate hydrate (C–S–H) gel, which contains internal, nanometer-scale gel pores that are an important aspect of its structure. Thus, as cement hydrates not only does the total porosity decrease, but the average pore size decreases by a few orders of magnitude. As a result, the permeability of cement paste is surprisingly low, typically lower than 1 nm^2 . Low permeability prevents the ingress of dissolved species, and is therefore an important characteristic for cement durability.

The C–S–H gel does not form with a fixed structure, but rather the morphology, surface area, and internal porosity can vary depending on the location within the specimen and also on environmental conditions. Microscopy of hardened pastes generally shows that a porous outer product morphology of C–S–H forms outside the perimeter of the cement grains (LD C–S–H), while a denser inner product morphology fills the volume originally occupied by the cement grains (HD C–S–H) [1]. The Jennings colloid model [2] proposes that C–S–H in mature paste forms with two packing densities of the same fundamental 5 nm C–S–H particles, resulting in interparticle gel pores

that are about 2 nm in size. This general picture is supported by a variety of experimental measurements including nanoindentation [3,4]. Hydrogen NMR relaxometry indicates that the pore system in cement hydrated at room temperature is bimodal, with characteristic pore sizes of $\sim 1\text{--}2 \text{ nm}$ and $10\text{--}30 \text{ nm}$ [5–7].

Curing cement paste at moderately elevated temperatures results in microstructural differences that are apparent from microscopy [8]. At higher temperatures the hydration product layers around the cement grains appear denser, and the microstructure appears less uniform, with a greater number of large (capillary) pores. This has been attributed to the formation of C–S–H gel with a smaller volume of gel pores [3,9].

This work is motivated in part by inconsistent results regarding the effect of curing temperature on the transport properties of hardened cement paste. Goto and Roy [10] measured the permeability of cement pastes cured at 20 °C and 60 °C using the standard pressure gradient method, and found that at a given water to cement mass ratio (w/c) the permeability after curing at 60 °C was at least an order of magnitude higher. The authors attributed the variation in permeability to a variation in the pore size distribution. Detwiler et al. [11] measured the rate of chloride diffusion (a parameter that depends in part on the permeability) of cement pastes cured at 5, 20, and 50 °C and found a more modest increase of a factor of 2 between 20 and 50 °C, but little change between 5 and 20 °C. In contrast, Marsh et al. [12] found that the permeability of neat cement paste cured at 20, 35, 50, and 65 °C did not exhibit a strong dependence on curing temperature, although there is a large amount of scatter in their data.

Conventional techniques for measuring permeability, like those used in the studies noted above, are cumbersome, time consuming,

^{*} Corresponding author. Tel.: +1 617 768 2346; fax: +1 617 768 2388.
E-mail address: jvalenza@slb.com (J.J. Valenza).

and markedly susceptible to experimental errors [13–15]. Therefore, the permeability measurement itself could be a major source of inconsistency. In the more recent past, the beam bending method, developed by Scherer [16,17], was applied to cement paste with good success [18–20]. This technique provides a consistent, convenient measure of the elastic and transport properties of a porous medium.

Here we revisit the effect of curing temperature on both the microstructure and properties of cement paste. The former is characterized by small angle neutron scattering (SANS) [3] and thermoporometry (TPM) [21], while the latter is characterized by beam bending. We utilize this information to provide insight into how the curing temperature affects the macroscopic properties via changes in the microstructure.

2. Experimental

2.1. Materials

All pastes were made with Type 1 OPC (Lafarge). For each batch, 900 g of cement was mixed with 405 g of water, giving $w/c = 0.45$. The paste was mixed by hand with a plastic spatula for 5 min and then poured into a plexiglas mold with four compartments, each with internal dimensions of 254 mm × 25 mm × 25 mm. The mold was tapped onto the counter for approximately 1 min to remove trapped air bubbles, and then sealed into a plastic container with a small amount of water at the bottom. For the pastes cured at 40 °C and 60 °C, the sealed mold was partially submerged in a circulating water bath. For the paste cured at 20 °C, the paste remained in the laboratory which was maintained at that temperature. The remaining batch was placed into a refrigerator which was maintained at 8 ± 1 °C. Pastes were demolded after 24 h (20, 40, 60 °C) or 48 h (8 °C) by disassembling the mold. The bars were then cured under lime water at the same temperature for an additional three months. After this time, all bars were stored at room temperature under the same saturated conditions until testing.

To form rectangular prismatic specimens for the beam bending experiments, the bars were cut lengthwise to thicknesses ranging from 3 mm to 7 mm using a water-lubricated diamond saw. Prior to the beam bending test, the specimens were pressurized at 3 MPa for 24 h while under lime water. This handling is necessary to ensure saturation of the pore system [18]. To determine the permeability and elastic modulus from the beam bending data it is necessary to measure the porosity (see Section 2.4). This parameter was inferred from the weight loss upon drying at 105 °C as measured on companion samples.

2.2. Small angle neutron scattering

The same cement paste specimens were analyzed using small angle neutron scattering (SANS). Thin (0.6 mm thick) specimens were cut from the rectangular bars using a water-lubricated wafering saw. After cutting the samples were stored and analyzed in the water-saturated state. The measurements were performed at the NIST Center for Neutron Research using the NIST/NSF NG3 30-m SANS instrument with a neutron wavelength of 0.8 nm. By varying the sample-to-detector distance, data for each specimen were obtained over a magnitude range of scattering vector of $0.02 < q < 3.0 \text{ nm}^{-1}$, where $q = 4\pi \sin(\phi/2)/\lambda$, ϕ is the angle of scatter, and λ is the neutron wavelength. Scattering from hydrated cement paste in this q -range is dominated by the interface between the solid nanoscale C–S–H hydration product and the pore fluid, i.e. the gel pores. In general, the upper limit in q for obtaining data from hydrating cement is about 2 nm^{-1} , due to the decrease in SANS intensity with increasing q .

For cement paste specimens it has previously been established that a Porod scattering regime exists at the highest accessible q

values, where the scattering arises almost entirely from the nanoscale C–S–H gel. In the range of $1.4 < q < 2.0 \text{ nm}^{-1}$ the scattering follows:

$$Int = \frac{C_p}{q^4} + BGD \tag{1}$$

where Int is the absolutely calibrated scattering intensity, C_p is the Porod constant, and BGD is incoherent scattering present as a flat (q -independent) background. The values of C_p and BGD are determined from a linear fit as shown in Fig. 1. The constant BGD value is subtracted from the scattering data to remove the flat background, while C_p is used to determine the specific surface area per unit specimen volume, S_T , according to:

$$S_T = \frac{C_p}{2\pi\Delta\rho^2} \tag{2}$$

where $\Delta\rho^2$, the neutron scattering contrast, is the square of the difference in the neutron scattering lengths of the phases generating the Porod scattering (solid C–S–H and water). The appropriate contrast for Eq. (2) was previously determined to be $9.74 \times 10^{28} \text{ m}^{-4}$ [22].

2.3. Thermoporometry

The pore systems of the cured cement pastes were also characterized using a cryogenic technique devised by Brun et al. [21] known as thermoporometry (TPM). This technique relies on the fact that a crystal confined in a small pore (i.e. <100 nm) melts at a lower temperature than a bulk crystal. The melting point depression is proportional to the curvature of the crystal/liquid interface, κ_{CL} , as described by the Gibbs–Thomson equation [23]:

$$\gamma_{CL}\kappa_{CL} = \int_T^{T_M} \Delta S_{Fv} dT \tag{3}$$

where T is the melting temperature of the confined crystal, T_M is the bulk melting point, γ_{CL} is the crystal/liquid interfacial energy, and ΔS_{Fv} is the entropy of fusion per unit volume of crystal. The curvature is governed by both the size, r_p , and geometry of the confining pore. For example, $\kappa_{CL} = 2/r_p$ for a hemispherical crystal/liquid interface, or $\kappa_{CL} = 1/r_p$ for a cylindrical interface.

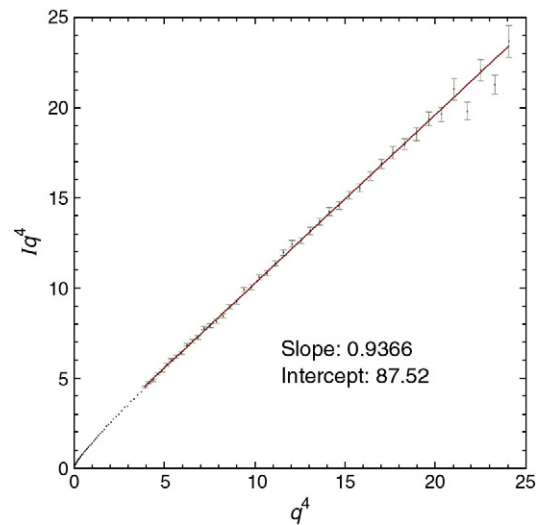


Fig. 1. Porod plot of the absolutely calibrated SANS data for cement paste hydrated at 20 °C. The solid line is a linear fit, for which the slope and intercept are given. The slope is the incoherent flat background scattering and the intercept is the Porod constant (see Eq. (1)).

Download English Version:

<https://daneshyari.com/en/article/1456800>

Download Persian Version:

<https://daneshyari.com/article/1456800>

[Daneshyari.com](https://daneshyari.com)